

Jet quenching in relativistic heavy ion collisions

Ivan Vitev

Los Alamos National Laboratory, Theory Division and Physics Division, Mail Stop H846
Los Alamos, NM 87545, USA

E-mail: ivitev@lanl.gov

Abstract.

Parton propagation in dense nuclear matter results in elastic, inelastic and coherent multiple soft scattering with the in-medium color charges. Such scattering leads to calculable modifications of the hadron production cross section that is evaluated in the framework of the perturbative QCD factorization approach. Final state medium-induced gluon bremsstrahlung is arguably the most efficient way of suppressing large transverse momentum particle production in nucleus-nucleus collisions. The observed hadronic attenuation, known as jet quenching, can be related to the properties of the medium, such as density and temperature, and carries valuable information about the early stages of heavy ion reactions. Non-Abelian energy loss in the quark-gluon plasma can be studied in much greater detail through the modification of the two particle back-to-back correlations. Perturbative calculations give good description of the redistribution of the lost energy in lower transverse momentum particles and predict significant increase of the correlation width of away-side di-hadrons. In contrast, energy loss in cold nuclear matter was found to be small but for large values of Feynman- x is expected to complement the dynamical higher twist shadowing in experimentally observable forward rapidity hadron suppression.

1. Energy loss in hot and dense nuclear matter

Jet quenching, the suppression of high transverse momentum hadron production relative to the expectation from p+p collisions scaled by the number of elementary nucleon-nucleon interactions, has been predicted [1] to be one of the key signatures for the creation of a hot and dense quark-gluon plasma (QGP) in ultra-relativistic nuclear collisions. Since, the non-Abelian energy loss of fast quarks and gluons in dense nuclear matter has been studied in great detail in a variety of theoretical approaches [2]. Its key features can be illustrated on the example of the reaction operator formalism [3], which systematically expands energy loss in terms of the correlations between multiple scattering centers.

For A+A collisions, the dominant final state energy loss follows the hard partonic scattering, which takes place on a time scale $t_0 \sim 1/Q$. Even in the absence of a medium, the large virtuality leads to non-Abelian bremsstrahlung. For real gluons of small and moderate frequencies ω [3]

$$|\mathcal{M}_c|^2 \propto \frac{dN_{\text{vac}}^g}{d\omega d\sin\theta^* d\delta} \approx \frac{C_R \alpha_s}{\pi^2} \frac{1}{\omega \sin\theta^*} . \quad (1)$$

In Eq. (1) $\theta^* = \arcsin(k_\perp/\omega)$ is the angle relative to the jet axis, δ is the azimuthal cone angle (both illustrated in right panel of Fig. 1), α_s is the strong coupling constant and $C_R = 3$ ($4/3$) for gluon (quark) jets, respectively. Virtual gluon corrections remove the $\omega \rightarrow 0$ infrared singularity in the cross sections in accord with the Kinoshita-Lee-Nauenberg theorem [4] but the collinear

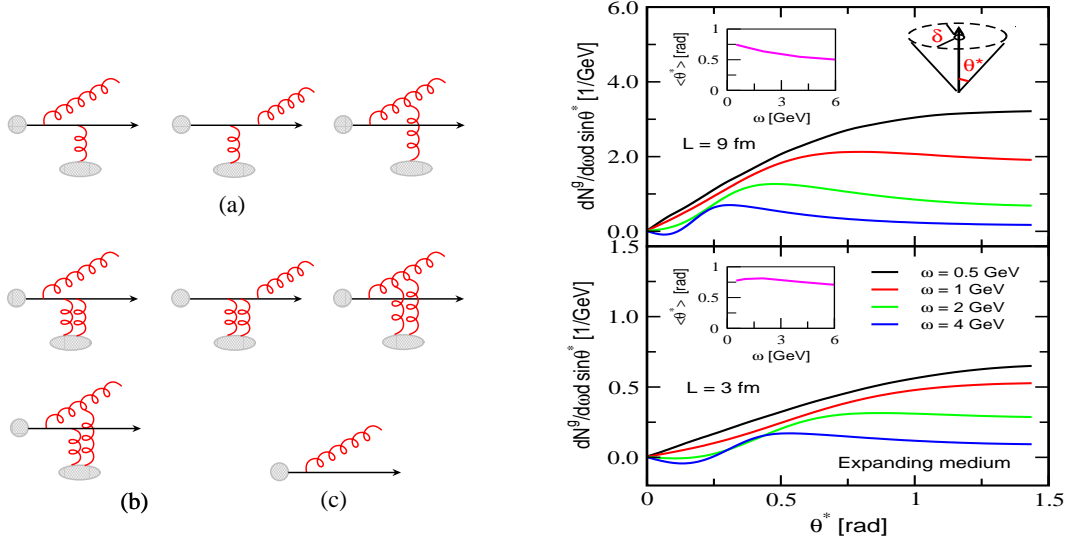


Figure 1. Left panel: diagrams contributing to the lowest order in opacity energy loss expansion. Right panel: the angular distribution of medium-induced bremsstrahlung of $E = 6 \text{ GeV}$ gluon jet for fixed values of the radiative gluon energy $\omega = 0.5, 1, 2, 4 \text{ GeV}$. Top and bottom panels represent (1+1)D Bjorken expanding medium of transverse size $L = 9 \text{ fm}$ and $L = 3 \text{ fm}$, respectively. Inserts show $\langle \theta^* \rangle$ versus ω .

$\theta^* \rightarrow 0$ divergence has to be regulated or subtracted in the parton distribution functions (PDFs) and the fragmentation functions (FFs).

In contrast, the final state medium-induced bremsstrahlung spectrum is both collinear and infrared safe. To first order in the mean number of soft interactions in the plasma the distribution of gluons in angle and frequency can be written as [5]

$$|\mathcal{M}_a|^2 + 2\text{Re}\mathcal{M}_b^\dagger \mathcal{M}_c \propto \frac{dN_{\text{med}}^g}{d\omega d\sin\theta^* d\delta} \approx \frac{2C_R\alpha_s}{\pi^2} \int_{z_0}^L \frac{d\Delta z}{\lambda_g(z)} \int_0^\infty dq_\perp q_\perp^2 \frac{1}{\sigma_{el}} \frac{d\sigma_{el}}{d^2q_\perp}(z) \int_0^{2\pi} d\alpha \frac{\cos\alpha}{q_\perp^2 - 2q_\perp\omega \sin\theta^* \cos\alpha + \omega^2 \sin^2\theta^*} \left[1 - \cos\left(\frac{(q_\perp^2 - 2q_\perp\omega \sin\theta^* \cos\alpha + \omega^2 \sin^2\theta^*)\Delta z}{2\omega} \right) \right]. \quad (2)$$

In Eq. (2) $\alpha = \angle(\vec{k}_\perp, \vec{q}_\perp)$, $\lambda_g(z)$ is the position-dependent gluon mean free path and L is the transverse size of the medium. The momentum transfers \vec{q}_\perp are distributed according to the normalized elastic scattering cross section $\sigma_{el}^{-1} d\sigma_{el}/d^2q_\perp(z) = \mu_D^2(z)/\pi(q_\perp^2 + \mu_D^2(z))^2$. In this model $\langle q_\perp^2 \rangle \propto \mu_D^2(z)$ and for a quark-gluon plasma in local thermal equilibrium $\mu_D^2(z) \sim 4\pi\alpha_s T^2$. For the case of (1+1)D dynamical Bjorken expansion of the QGP $\mu_D(z) = \mu_D(z_0)(z_0/z)^{1/3}$, $\lambda_g(z) = \lambda_g(z_0)(z/z_0)^{1/3}$. At small angles θ^* both the direct and double Born terms [3] in Eq. (2) are divergent. However, they come with different signs $\propto (-i)^2 = -1$, $\propto i(-i) = 1$, equivalent to a phase difference π . The soft and collinear divergences then exactly cancel [5].

From Eq. (2) the gluon distribution is not only finite when $\theta^* \rightarrow 0$ but vanishes on average due to the uniform angular distribution of momentum transfers from the medium, $\int_0^{2\pi} d\alpha \cos\alpha = 0$. We have checked that for physical gluons of $k_\perp \leq \omega$ the cancellations discussed here persist to all orders in the mean number of scatterings [3]. The small frequency and small angle spectral behavior of $dN_{\text{med}}^g/d\omega d\sin\theta^* d\delta$ remains under perturbative control. Given the vastly different

angular behavior of the vacuum and the medium-induced gluon bremsstrahlung, Eqs. (1) and (2), it is critical to identify the phase space where cancellation of the color currents induced by the hard and soft scattering occurs. We fix the parameters of the medium to $\mu_D(z_0) = 1.5$ GeV and $\lambda_g(z_0) = 0.75$ fm at initial formation time $z_0 = 0.25$ fm. Since small frequency emission is suppressed, we use only a moderate $\alpha_s = 0.25$. Triggering on high p_{T1} hadron directs its parent parton “c” away from the medium and places the collision point of the lowest order (LO) $ab \rightarrow cd$ underlying perturbative process [6] close to the periphery of the nuclear overlap region. Then, it is the back-scattered jet “d” that traverses the QGP. For large nuclei, such as Au and Pb, path lengths $L = 9$ (3) fm are used to illustrate central (peripheral) collisions, respectively. We limit gluon emission to the forward jet hemisphere, $0 \leq \theta^* \leq \frac{\pi}{2}$.

The angular distribution of medium-induced radiation for $E = 6$ GeV gluon jet for select values of ω is shown in Fig. 1. We find that gluon emission is strongly suppressed within a cone of opening angle $\theta^* \simeq 0.25$ rad. The broad gluon distribution can be characterized by the mean emission angle

$$\langle \theta^* \rangle = \int_0^1 \theta^* \frac{dN_{\text{med}}^g}{d\omega d\sin\theta^*} d\sin\theta^* \left[\int_0^1 \frac{dN_{\text{med}}^g}{d\omega d\sin\theta^*} d\sin\theta^* \right]^{-1},$$

given in the insert of Fig. 1. We emphasize that the angular spectrum is distinctly non-Gaussian and the mechanism that determines its form is based on the destructive interference of color currents from hard and soft parton scattering rather than a slow random walk of the gluon in θ^* . The large angle distribution or radiative quanta is evident for both large and small frequencies ω .

In the case of heavy quark creation and propagation the vacuum [7] and the Bertsch-Gunion radiation [8] are modified by the large mass M_q . The mass enters in the propagators as follows, $k_{\perp}^2 \rightarrow k_{\perp}^2 + \omega^2 M_q^2 / E^2$, and suppresses the gluon bremsstrahlung for $\sin\theta^* \leq M_q/E$. Such depletion can only be effective if gluon radiation peaks at $\theta^* \rightarrow 0$. Since for light quarks the final state medium-induced non-Abelian bremsstrahlung is *not* dominated by small angle emission, see left panel of Fig. 1, effects other than the “dead cone” control the energy loss pattern of heavy versus light quarks.

Qualitatively, for light quarks the behavior of the energy loss as a function of the density and the size of the system can be summarized to first order in opacity as follows:

$$\begin{aligned} \Delta E &\approx \int dz \frac{C_R \alpha_s \mu^2}{2 \lambda_g} z \ln \frac{2E}{\mu^2 L} = \int dz \frac{9 C_R \pi \alpha_s^3}{4} \rho^g(z) \ln \frac{2E}{\mu^2 L} \\ &= \begin{cases} \frac{9 C_R \pi \alpha_s^3}{8} \rho^g L^2 \ln \frac{2E}{\mu^2 L}, & \text{static} \\ \frac{9 C_R \pi \alpha_s^3}{4} \frac{1}{A_{\perp}} \frac{dN^g}{dy} L \ln \frac{2E}{\mu^2 L}, & (1+1)D \end{cases} \end{aligned} \quad (3)$$

Eq. (3) assumes energetic jets and neglects kinematic bounds. Here, A_{\perp} is the transverse size of nuclear matter. For static systems ΔE depends quadratically on the nuclear size. For the case of longitudinal Bjorken expansion this dependence is reduced to linear [3] but the energy loss is sensitive to the initial parton rapidity density dN^g/dy . Understanding the effective color charge density dependence of ΔE is the key to jet tomography [9].

The calculated energy loss can be incorporated in the perturbative QCD factorization approach as a modification of the single and double inclusive hadron production cross sections. To lowest order in the double collinear limit these are given by:

$$\begin{aligned} \frac{d\sigma_{NN}^{h_1}}{dy_1 dp_{T1}} &= K \sum_{abcd} p_{T1} \int \frac{dz_1}{z_1^2} D_{h_1/c}(z_1) \int dx_a \frac{\phi_{a/N}(x_a) \phi_{b/N}(x_b)}{x_a x_b S} \left[\frac{1}{x_a S + U/z_1} \right] \\ &\times 2\pi \alpha_s^2 |\overline{M}_{ab \rightarrow cd}|^2, \end{aligned} \quad (4)$$

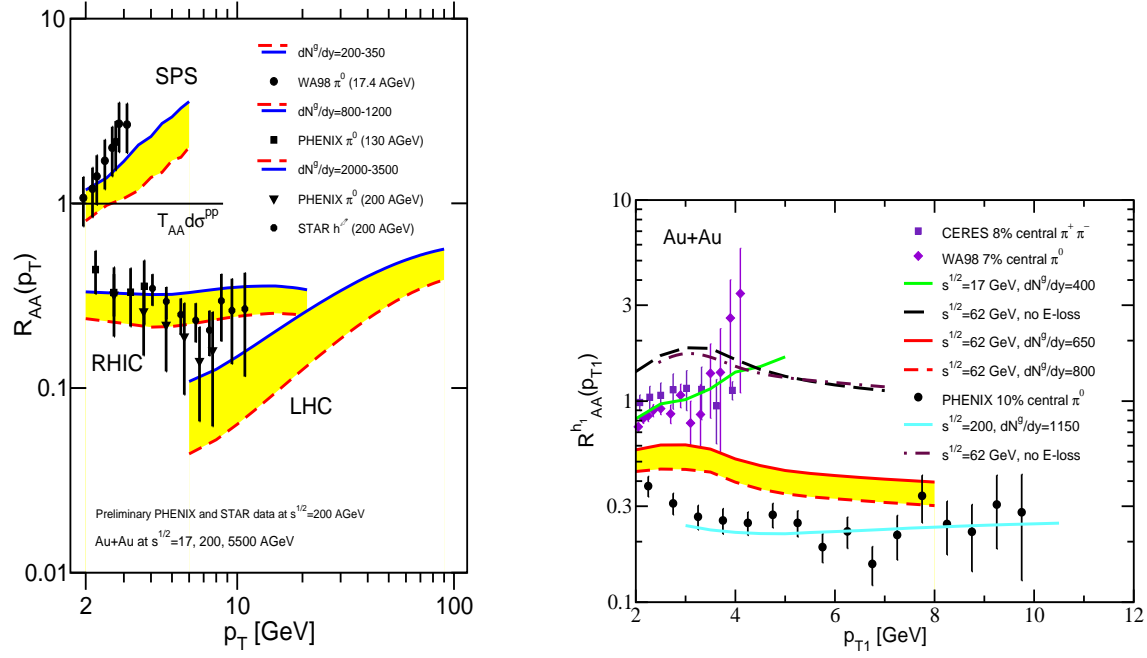


Figure 2. Left panel: nuclear modification factor $R_{AA}^{h_1}(p_T)$ for single inclusive pion production at SPS, RHIC and the LHC. Right panel: the same nuclear modification for the RHIC Au+Au run at c.m. energy of 62 AGeV.

$$\begin{aligned} \frac{d\sigma_{NN}^{h_1 h_2}}{dy_1 dy_2 dp_{T1} dp_{T2} d\Delta\varphi} &= K \sum_{abcd} \int \frac{dz_1}{z_1} D_{h_1/c}(z_1) \left[D_{h_2/d}(z_2) \delta(\Delta\varphi - \pi) \right] \frac{\phi_{a/N}(x_a) \phi_{b/N}(x_b)}{x_a x_b S^2} \\ &\times 2\pi \alpha_s^2 |\overline{M}_{ab \rightarrow cd}|^2. \end{aligned} \quad (5)$$

In Eq. (5) $K = 2$ is a next-to-leading order K -factor, $x_{a,b} = p_{a,b}/p_{N_a, N_b}$ are the momentum fractions of the incoming partons and $z_{1,2} = p_{h_1, h_2}/p_{c,d}$ are the momentum fractions of the hadronic fragments. We use standard lowest order Gluck-Reya-Vogt PDFs [10] and Binnewies-Kniehl-Kramer FFs [11]. Renormalization, factorization and fragmentation scales are suppressed everywhere for clarity. The spin (polarization) and color averaged matrix elements $|\overline{M}_{ab \rightarrow cd}|^2$ are given in [6].

Dynamical nuclear effects in multi-particle production can be studied through the ratio [12]

$$R_{AB}^{(n)} = \frac{d\sigma_{AB}^{h_1 \dots h_n} / dy_1 \dots dy_n d^2 p_{T1} \dots d^2 p_{Tn}}{\langle N_{AB}^{\text{coll}} \rangle d\sigma_{NN}^{h_1 \dots h_n} / dy_1 \dots dy_n d^2 p_{T1} \dots d^2 p_{Tn}}. \quad (6)$$

Centrality dependence is implicit in Eq. (6) and the modified cross section per average collision $d\sigma_{AB}^{h_1 \dots h_n} / \langle N_{AB}^{\text{coll}} \rangle$ can be calculated from Eqs. (4) and (5) including the numerically evaluated energy loss. Calculation of the nuclear modification in central Au+Au collisions [9] at $\sqrt{s_{NN}} = 17, 200, 5500$ GeV are shown in the left panel of Fig. (1). The right panel of Fig. (1) extends the GLV jet quenching predictions [13] to the intermediate RHIC energy of $\sqrt{s_{NN}} = 62$ GeV. In this case parton energy loss, driven by the medium density dN^g/dy , is smaller but its effect at high p_T is amplified by the steepness of the underlying partonic spectra. Similar results for the light pion suppression were found in [14]. Baryons, however, are expected to be significantly less suppressed. In fact, the p/π^+ ratio was predicted to be larger than at the

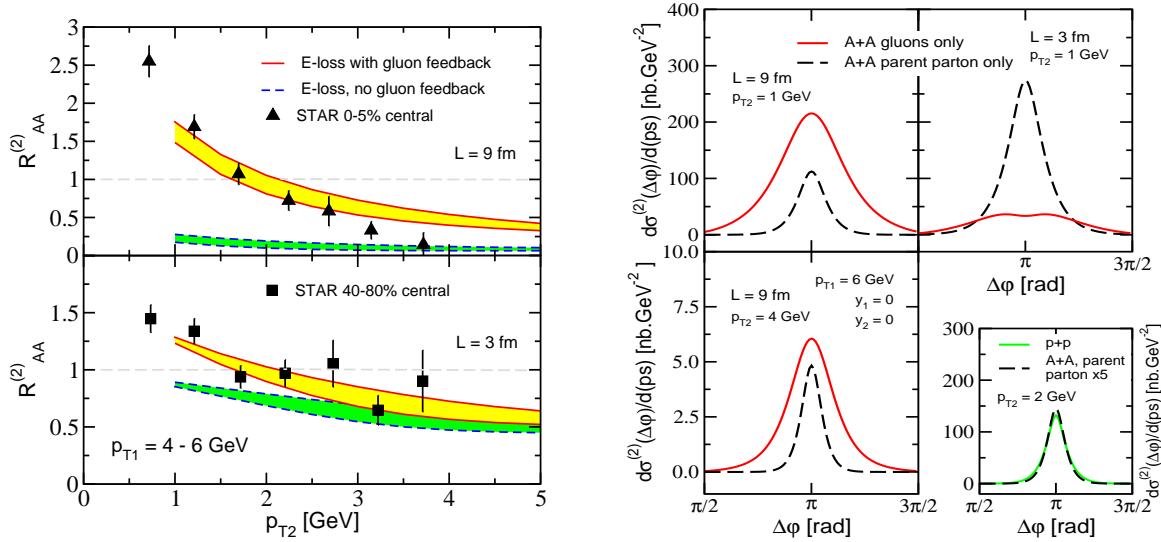


Figure 3. Left panel: nuclear modification $R_{AA}^{(2)}(p_{T1}, p_{T2})$ in central and peripheral Au+Au collisions at RHIC of the back-to-back di-hadron correlations with and without the contribution of medium-induced bremsstrahlung. Right panel: angular correlations of hadrons dominated by large angle gluon emission. Solid and dashed lines give *separately* the contribution of the radiative gluons and the attenuated parent parton.

top RHIC energy [15]. Relating the observed high p_T hadron attenuation [16, 17, 18, 19] to the energy density in central Au+Au collisions through the assumption of local thermal equilibrium we find that at times $\tau_0 \simeq 0.6$ fm $\epsilon_0 \simeq 15 - 20$ GeV/fm³ at $\sqrt{s_{NN}} = 200$ GeV, well in excess of the critical energy for deconfinement ($\epsilon_c \simeq 1$ GeV/fm³).

More detailed information about the properties of the quark-gluon plasma can be extracted via two particle correlation analysis. At present, a key question for perturbative QCD phenomenology is whether the medium induced gluon bremsstrahlung can significantly alter the di-hadron correlations measured at RHIC [20, 21]. We naturally focus on the away-side $|\Delta\varphi| \geq \frac{\pi}{2}$ case, where medium effects are the largest. A modification that does not change the $\Delta\varphi$ -integrated cross section is vacuum- and medium-induced acoplanarity. The deviation of jets from being back-to-back in a plane perpendicular to the collision axis arises from the soft gluon radiation and transverse momentum diffusion in dense nuclear matter [22]. In the approximation of collinear fragmentation, the width of the away-side hadron-hadron correlation function can be related to the accumulated di-jet transverse momentum squared in the φ -plane, $\sin \sqrt{\frac{2}{\pi}} \sigma_{\text{Far}} = \sqrt{\frac{2}{\pi}} \langle k_T^2 \rangle_{\varphi} / p_{\perp d}$. Assuming a Gaussian form,

$$f_{\text{vac. or med.}}(\Delta\varphi) = \frac{1}{\sqrt{2\pi}\sigma_{\text{Far}}} e^{-\frac{(\Delta\varphi - \pi)^2}{2\sigma_{\text{Far}}^2}}, \quad (7)$$

a good description of $|\Delta\varphi| \geq \frac{\pi}{2}$ correlations measured in elementary p+p collisions at $\sqrt{S} = 200$ GeV [18] requires a large $\langle k_T^2 \rangle_{\text{vac}} = 5$ GeV² for the di-jet pair with away-side scattered quark (and a 2.25 larger value for a scattered gluon). Additional broadening arises from the interactions of the jet in the QGP that ultimately lead to the reported energy loss, $\langle k_T^2 \rangle_{\text{hot}} = 2\mu_D^2(z_0)/\lambda_{q,g}(z_0) \ln \frac{L}{z_0}$, although only half is projected on the φ -plane, $\langle k_T^2 \rangle_{\varphi} = \langle k_T^2 \rangle_{\text{vac}} + \frac{1}{2} \langle k_T^2 \rangle_{\text{hot}}$.

Two competing mechanisms do, however, change the p_{T2} dependence of the perturbative cross section, Eq. (5). First is the the parent jet “d” fractional energy loss $\epsilon = \Delta E_d/E_d$, which we here

for simplicity consider on average and evaluate by integrating Eq. (2). It leads to a rescaling of the hadronic fragmentation momentum fraction $z_2 \rightarrow z_2/(1-\epsilon)$ [2]. If the energy loss is large, a second mechanism is invoked as a consequence. Hadronic fragments of the radiative gluons will increase the probability of finding low and moderate p_{T_2} particles associated with the interacting jet [23].

To calculate di-hadron correlations, we first map the jet structure of a hard 90° -scattered parton on rapidity $y \approx \eta = -\ln \tan(\theta/2)$ (θ being the angle relative to the beam axis) and azimuth ϕ ,

$$\tan^2 \theta^* = \cot^2 \theta + \tan^2 \phi, \quad \tan \delta = -\frac{\cot \theta}{\tan \phi}, \quad \left| \frac{\partial(\sin \theta^*, \delta)}{\partial(\theta, \phi)} \right| = \frac{1}{\sin^2 \theta \cos^2 \phi} \frac{(\tan^2 \phi + \cot^2 \theta)^{-1/2}}{(1 + \tan^2 \phi + \cot^2 \theta)^{3/2}}.$$

The approximately flat rapidity distribution of the away-side jet near $y_2 = 0$ can be used to sum over all emission angles $\theta \in (\theta_{\min}, \theta_{\max}) \subset (0, \pi)$ yielding

$$\frac{dN_{\text{med}}^g}{d\omega d\phi} = \int_{\theta_{\min}}^{\theta_{\max}} d\theta \left[\frac{dN_{\text{med}}^g}{d\omega d\sin \theta^* d\delta} \left| \frac{\partial(\sin \theta^*, \delta)}{\partial(\theta, \phi)} \right| \right]. \quad (8)$$

It is critical to note that projection on a plane coincident with the jet cone axis (the ϕ -plane in Eq. (8) is one example) efficiently masks the $\theta^* \rightarrow 0$ void in the angular distribution of medium-induced gluons reported in Fig. 1. Our conclusion is independent of the physical mechanism that depletes the parton (or particle) multiplicity in a cone around the jet axis.

The end analytic result for the modification to Eq. (5) per average nucleon-nucleon collision in the heavy ion environment can be derived from the energy sum rule for all hadronic fragments from the jet,

$$\begin{aligned} D_{h_2/d}(z_2) \delta(\Delta\varphi - \pi) &\Rightarrow \frac{1}{1-\epsilon} D_{h_2/d} \left(\frac{z_2}{1-\epsilon} \right) f_{\text{med.}}(\Delta\varphi) + \frac{p_{T_1}}{z_1} \int_0^1 \frac{dz_g}{z_g} D_{h_2/g}(z_g) \\ &\times \int_{-\pi/2}^{\pi/2} d\phi \frac{dN_{\text{med}}^g(\phi)}{d\omega d\phi} f_{\text{vac.}}(\Delta\varphi - \phi). \end{aligned} \quad (9)$$

Here, $z_g = p_{T_2}/\omega$.

Numerical results, shown in the left panel of Fig. 3, correspond to triggering on a high $p_{T_1} = 4 - 6$ GeV pion and measuring all associated $\pi^+ + \pi^0 + \pi^-$. Depletion of hadrons from the quenched parent parton alone leads to a large suppression of the double inclusive cross section – a factor of 5 - 10 in central and a factor of 1.5 - 2 in peripheral reactions with weak p_{T_2} dependence. Hadronic feedback from the medium-induced gluon radiation, however, completely changes the nuclear modification factor $R_{AA}^{(2)}$. It now shows a clear transition from a quenching of the away-side jet at high transverse momenta to enhancement at $p_{T_2} \leq 2$ GeV, a scale significantly larger than the one found in [23]. STAR data in central and peripheral Au+Au collisions [20] is shown for comparison.

Two-particle distributions in A+A reactions, calculated from Eqs. (5) and (9) for a $p_{T_1} = 6$ GeV trigger pion and two different $p_{T_2} = 1, 4$ GeV associated pions, are shown in the Fig. (3). Qualitatively, the medium-induced gluon component to the cross section controls the growth of the correlation width in central and semi-central nuclear collisions. Quantitatively, the effect should be even larger than the one estimated here, which is limited by the imposed $0 < \theta^* < \frac{\pi}{2}$ constraint. Experimental measurements of significantly enhanced widths for $|\Delta\varphi| \geq \frac{\pi}{2}$ two-particle correlation in A+A collisions should thus point to copious hadron production from medium-induced large angle gluon emission.

2. Dynamical shadowing and energy loss in cold nuclear matter

Single and double inclusive hadron production in reactions involving nuclei is also modified by dynamical shadowing effects. Suppression of the particle production rates arises from the coherent final state scattering of the struck small- x parton with several nucleons and the generation of dynamical parton mass $m_{dyn}^2 = \xi^2 A^{1/3}$. Here, $\xi^2 = 0.09 - 0.12 \text{ GeV}^2$ for quarks is the scale of higher twist extracted from deeply inelastic scattering in heavy targets [24]. For electroweak vector meson exchange processes in DIS resumming the power corrections leads to an effective rescaling in the values of Bjorken- x . For p+A and A+A reactions the dynamical mass is amplified for the case of final state gluon scattering by the Casimir ratio $C_A/C_F = 2.25$. It leads to significantly larger power correction effects in hadronic reactions. Effectively,

$$x_B \rightarrow x_B \left(1 + \frac{\xi^2 (A^{1/3} - 1)}{Q^2} \right), \quad x \rightarrow x \left(1 + \frac{C_d \xi^2 (A^{1/3} - 1)}{-\hat{t}} \right), \quad (10)$$

where the normalization relative to the proton is already included in Eq. (10) and $C_d = 1$ (2.25) for quarks (gluons) respectively.

The left panel of Fig. 4 shows the nuclear modification $R_{dA}(p_T)$ for hadron production in d+Au reactions [12]. We emphasize that the effect is large at small p_T and relatively small at high p_T . Note that at forward rapidity in Eq. (10) $-\hat{t} = p_T^2$. Data on forward y hadron production from BRAHMS is also shown [25]. The right panel of Fig. 4 presents the broadening and attenuation of the two particle back-to-back correlations. Such effects are found to be large at forward rapidity and at small p_{T1}, p_{T2} [12]. The coherent multiple scattering discussed here take place (in the c.m. of the collision) over a short interval $t \sim R_A/\gamma \ll R_A$ and for the case of A+A reactions precedes and complements the energy loss in the QGP which develops at time scales $t \sim R_A$.

In cold nuclear matter energy loss is anticipated to be significantly smaller when compared to the one in the quark-gluon plasma. It has been experimentally verified through measurements in $d + Au$ reactions at RHIC at $\sqrt{s_{NN}} = 200 \text{ GeV}$ where a small enhancement consistent with Cronin multiple scattering [26] has been observed [27]. It has been argued, however, that the radiative energy loss induced by the scattering of fast on-shell partons in nuclear matter evaluated by Bertsch and Gunion [28] can be implemented as a ‘‘Sudakov’’ suppression factor $S(x_F) \approx 1 - x_F$ [29] and can give a good description of the A^α , $\alpha < 1$ suppression in a large class of observed cross sections in hadronic reactions at forward x_F .

3. Conclusions

In summary, we calculated the nuclear modification of inclusive moderate and high p_T particle production and the back-to-back particle correlations in the framework of the perturbative QCD factorization approach, augmented by inelastic jet interactions in the quark-gluon plasma. Jet tomographic analysis of hadron attenuation points to initial energy density of $15 - 20 \text{ GeV/fm}^3$ in $\sqrt{s_{NN}} = 200 \text{ GeV}$ central Au+Au collisions. At RHIC energies we found that the medium-induced gluon radiation determines the $|\Delta\phi| \geq \frac{\pi}{2}$ two-particle yields and the width of their correlation function to surprisingly high transverse momentum $p_{T2} \sim 10 \text{ GeV}$. The predicted transition from back-to-back jet enhancement to back-to-back jet quenching is quantitatively compatible with the recent STAR data. In cold nuclear matter at RHIC coherent final state multiple scattering gives the dominant contribution to the attenuation of single and double inclusive hadron production. Energy loss, however, may also play an important role at forward x_F .

Acknowledgments: This work is supported by the J. R. Oppenheimer Fellowship of the Los Alamos National Laboratory and by the US Department of Energy.

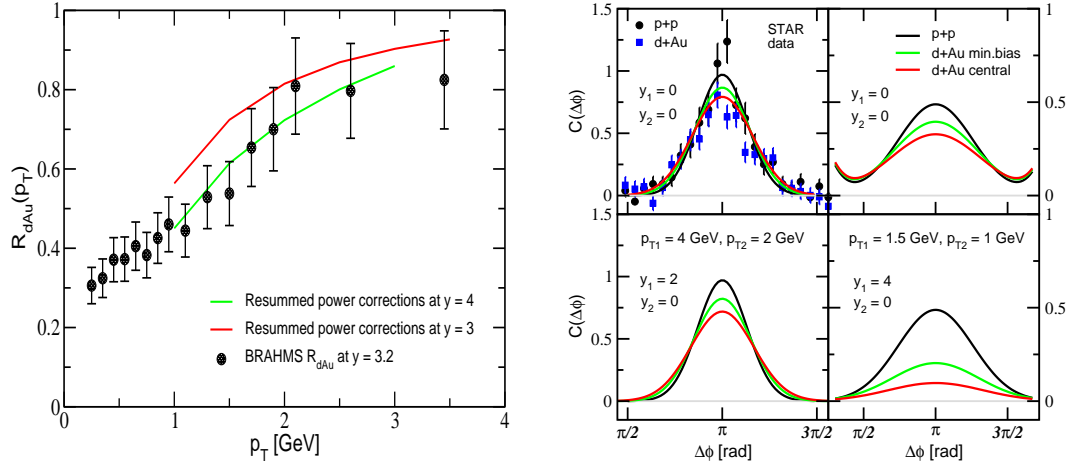


Figure 4. Left panel: modification of the single inclusive hadron production from resummed nuclear enhanced power corrections in forward rapidity d+Au collisions at RHIC. Right panel: modification of the back-to-back di-hadron correlations versus rapidity, centrality and p_T in $\sqrt{s_{NN}} = 200$ GeV d+Au reactions.

References:

- [1] X. N. Wang and M. Gyulassy, Phys. Rev. Lett. **68**, 1480 (1992).
- [2] M. Gyulassy *et al.*, nucl-th/0302077; A. Kovner and U. A. Wiedemann, hep-ph/0304151; R. Baier *et al.*, Ann. Rev. Nucl. Part. Sci. **50**, 37 (2000).
- [3] M. Gyulassy, P. Levai and I. Vitev, Nucl. Phys. B **594**, 371 (2001); Phys. Rev. Lett. **85**, 5535 (2000); Nucl. Phys. B **571**, 197 (2000); M. Djordjevic and M. Gyulassy, Nucl. Phys. A **733**, 265 (2004).
- [4] T. Kinoshita, J. Math. Phys. **3**, 650 (1962); T. D. Lee, M. Nauenberg, Phys. Rev. **133**, B1549 (1964).
- [5] I. Vitev, hep-ph/0501255.
- [6] J. F. Owens, Rev. Mod. Phys. **59**, 465 (1987).
- [7] Y. L. Dokshitzer, V. A. Khoze and S. I. Troian, Phys. Rev. D **53**, 89 (1996).
- [8] R. Thomas, B. Kampfer and G. Soff, hep-ph/0405189.
- [9] I. Vitev, M. Gyulassy, Phys. Rev. Lett. **89**, 252301 (2002); I. Vitev, J. Phys. G **30**, S791 (2004), references therein.
- [10] M. Gluck, E. Reya, A. Vogt, Eur. Phys. J. C **5**, 461 (1998).
- [11] J. Binnewies, B. A. Kniehl, G. Kramer, Z. Phys. C **65**, 471 (1995).
- [12] J. W. Qiu, I. Vitev, hep-ph/0405068.
- [13] I. Vitev, Phys. Lett. B **606**, 303 (2005).
- [14] A. Adil and M. Gyulassy, Phys. Lett. B **602**, 52 (2004); X. N. Wang, Phys. Rev. C **70**, 031901 (2004).
- [15] V. Greco, C. M. Ko and I. Vitev, Phys. Rev. C in press, nucl-th/0412043.
- [16] P. Levai *et al.*, Nucl. Phys. A **698**, 631 (2002).
- [17] K. Adcox *et al.*, Phys. Rev. Lett. **88**, 022301 (2002); S. S. Adler *et al.*, Phys. Rev. Lett. **91**, 072301 (2003).
- [18] J. Adams *et al.*, Phys. Rev. Lett. **91**, 072304 (2003).
- [19] Z. b. Xu, nucl-ex/0411001; H. Busching, nucl-ex/0410002.
- [20] C. Adler *et al.*, Phys. Rev. Lett. **90**, 082302 (2003). J. Adams *et al.*, nucl-ex/0501016;
- [21] J. Rak, J. Phys. G **30**, S1309 (2004).
- [22] J. W. Qiu, I. Vitev, Phys. Lett. B **570**, 161 (2003); P. Levai, G. Fai and G. Papp, hep-ph/0502238.
- [23] S. Pal, S. Pratt, Phys. Lett. B **574**, 21 (2003).
- [24] J. W. Qiu and I. Vitev, Phys. Rev. Lett. **93**, 262301 (2004); Phys. Lett. B **587**, 52 (2004).
- [25] I. Arsene *et al.*, nucl-ex/0403005.
- [26] Y. Zhang, *et al.* Phys. Rev. C **65**, 034903 (2002); I. Vitev, Phys. Lett. B **562**, 36 (2003).
- [27] I. Arsene *et al.*, Phys. Rev. Lett. **91**, 072305 (2003); S. S. Adler *et al.*, Phys. Rev. Lett. **91**, 072303 (2003); B. B. Back, Phys. Rev. Lett. **91**, 072302 (2003).
- [28] J. F. Gunion and G. Bertsch, Phys. Rev. D **25**, 746 (1982).
- [29] B. Z. Kopeliovich *et al.*, hep-ph/0501260.